Real-Time Observation of Single Atoms Trapped and Interfaced to a Nanofiber Cavity

Kali P. Nayak, Jie Wang, and Jameesh Keloth

Phys. Rev. Lett. **123**, 213602 — Published 19 November 2019

DOI: 10.1103/PhysRevLett.123.213602

Real-time observation of single atoms trapped and interfaced to a nanofiber cavity

Kali P. Nayak[†⋆], Jie Wang[†‡], and Jameesh Keloth
Center for Photonic Innovations and Institute for Laser Science, University of Electro-Communications, Chofu-shi, Tokyo 182-8585

We demonstrate efficient interfacing of individually trapped single atoms to a nanofiber cavity. The cavity is formed by fabricating photonic crystal structures directly on the nanofiber using femtosecond laser ablation. The single atoms are interfaced to the nanofiber cavity using an optical tweezer based side-illumination trapping scheme. We show that the fluorescence of individual single atoms trapped on the nanofiber cavity can be readily observed in real-time through the fiber guided modes. From the photon statistics measured for different cavity decay rates, the effective coupling rate of the atom-cavity interface is estimated to be 34±2 MHz. This yields a cooperativity of 5.4±0.6 (Purcell factor = 6.4±0.6) and a cavity enhanced channeling efficiency as high as 85±2% for a cavity mode with a finesse of 140. The trap lifetime is measured to be 52±5 ms. These results may open new possibilities for deterministic preparation of single atom events for quantum photonics applications on an all-fiber platform.

Realization of an efficient quantum interface will enable deterministic quantum state-transfer between atoms and photons for quantum information processing [1]. In this direction, there have been significant advances towards deterministic interfacing of trapped single atoms to tightly confined photonic modes in optical resonators [2]. From the viewpoint of a quantum network [1], fiber-coupled quantum interfaces will be promising candidates for quantum nodes [3–6].

In this context, tapered optical nanofiber (ONF) based cavity provides a unique fiber-in-line platform for cavity quantum electrodynamics (QED) [7, 8]. Due to the strong transverse confinement of the ONF guided modes, even a moderate finesse ONF cavity can enable high single atom cooperativity [7, 8]. Moreover, based on the achievable finesse, the cavity parameters can be designed by choosing appropriate cavity length ranging from tens of microns to few meters [7–9]. Based on this concept, strong-coupling regime of cavity QED has been demonstrated using a 33 cm long ONF cavity with a finesse <40, realized by sandwiching the tapered fiber between two conventional fiber Bragg mirrors [10]. However, the extremely long cavity length and the presence of the tapered section within the cavity, limit the atom-cavity coupling rate ($2\pi \times 7.4$ MHz) and the achievable cooperativity (~ 3.3) [8, 10].

In recent years, there have been significant development for fabricating high quality photonic crystal (PhC) structures directly on the ONF using femtosecond laser ablation technique [9, 11, 12]. This leads to designable cavity lengths of few to several millimeters, enabling fiber-in-line cavity operation in both Purcell and strong-coupling regime with high atom-cavity coupling rate and high cooperativity [8, 9].

On the other hand, in order to trap atoms in the vicinity of the ONF, the only scheme demonstrated so far is the two-color guided mode trap [10, 13–15]. However, the scheme lacks the control over atom number and position. In this context, real-time observation [5] and individually controlled single atoms [3, 4] efficiently interfaced to a photonic mode will be crucial requirements for deterministic quantum gate operations.

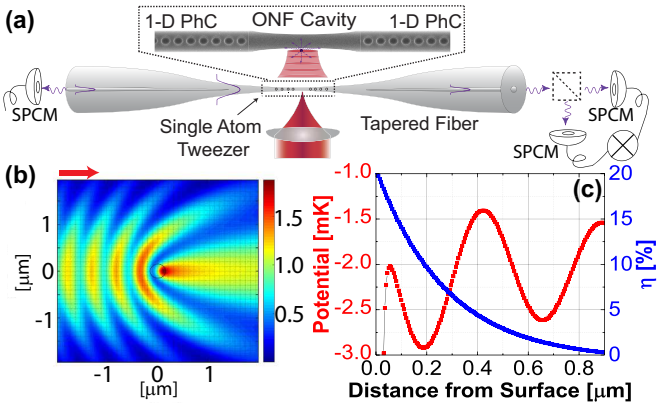

FIG. 1. (Color Online) Optical tweezer based side-illumination ONF trap. (a) Schematic diagram of the experiment. (b) Intensity distribution of the tweezer beam around the ONF estimated using FDTD simulation. The black circle at the center indicates the ONF position and the red arrow shows the irradiation direction. (c) The estimated trapping potential (red squares) and the corresponding η (blue squares) plotted as a function of radial separation from the fiber surface, for a fiber diameter of 300 nm.

Here, we demonstrate an optical tweezer based side-illumination trapping scheme to trap and efficiently interface individual single atoms to a few millimeter-long ONF cavity fabricated directly on the ONF. We show that the fluorescence of single atoms trapped on the ONF cavity can be readily observed in real-time through the fiber guided modes. The effective coupling rate of the atom-cavity interface is estimated to be 34±2 MHz. This yields a cooperativity of 5.4±0.6 (Purcell factor = 6.4±0.6) and a cavity enhanced channeling efficiency as high as 85±2% for a cavity mode with a finesse of 140.

A schematic diagram of the experiment is shown in Fig. 1(a). The ONF cavity is formed by fabricating two photonic crystal (PhC) structures on the ONF using femtosecond laser ablation [9, 11, 12]. Single atoms are trapped on the ONF segment between the two PhCs.

The dipole trap beam is tightly focused on the ONF and forms an optical tweezer for single atoms. When the tweezer beam hits the ONF, it forms standing-wave like nanotraps close to ONF due to the interference of the incident and the reflected lights from the fiber surface. The fluorescence of trapped single atom coupled to the ONF cavity mode are detected at the either ends of the fiber using single photon counting modules (SPCMs).

Figure 1(b) shows the typical intensity distribution of the tweezer beam around the ONF estimated using finite difference time domain (FDTD) simulation. The black circle at the center indicates the ONF position. The ONF diameter used for the simulation is 300 nm. The tweezer beam with a wavelength of 938 nm (red-detuned magic wavelength for Cs-atom [14]) is focused to 1 μm beam waist and is irradiated perpendicular to the ONF from the left side. The polarization is chosen to be parallel to the fiber axis. It may be seen that standing-wave like intensity pattern is formed in the irradiation-side, resembling an 1-D optical lattice. The first lattice site nearest to the fiber surface enables tight localization of the trap along the radial direction of the ONF. The tightly focused tweezer beam enables localization of the trap along the axial and azimuthal direction of the ONF.

For a given trapping laser wavelength, the position of the first lattice site depends on the fiber diameter. The channeling efficiency (η) of spontaneous emission of atom into ONF guided modes (a measure of the interaction strength) also depends on the ONF diameter and the radial position of atom from the ONF [16]. Therefore the selection of ONF diameter, is a crucial design principle for the efficient interfacing of the trapped atom with the ONF guided modes. From the theoretical simulations, we have found that ONF diameter of around 300 nm gives the optimum conditions for both trap depth and η (see Supplementary Material [17]).

Figure 1(c) shows the trapping potential (including the van der Waals potential) estimated assuming a beam waist of 1 μm and a power of 14 mW [13] and the corresponding η estimated for the excited state ($6P_{3/2}|F = 5, m_F = 5\rangle$) of the Cs-atom D2-transition [16] for a 300 nm diameter fiber plotted as a function of radial distance from the fiber surface. It may be seen that the closest trapping minimum is created at $\simeq$ 190 nm from the fiber surface with a trap depth of $\simeq$ 0.9 mK and η of 10.0% can be realized at the trap position. The trap frequencies along the radial and axial direction of the ONF are estimated to be $2\pi\times$(380 and 80) kHz, respectively. It should be noted that the η at the second lattice site is only 1.4%.

In the experiment, we have used an ONF cavity that has a central ONF segment with a diameter of 300±10 nm [17]. From the measured free spectral range ($\Delta\nu_{FSR} = 23 \pm 2$ GHz), the optical path length (L) of the cavity is estimated to be 6.5±0.5 mm. The ONF cavity modes have linewidths ($\Delta\nu$ = FWHM of the cavity transmission peaks) in the range 150-1200 MHz and can be tuned to the Cs-atom resonance by stretching the tapered fiber using a piezo actuator (Attocube, ANPx51) attached to the fiber holder. The dipole trap beam is tightly focused to 1 μm beam waist using a high numerical aperture ($NA = 0.5$) lens introduced into the vacuum chamber, forming an optical tweezer for single atoms. The tweezer spot is aligned to the ONF by monitoring the tweezer light scattered into the ONF guided modes [17]. A blue-detuned laser light with a wavelength of 830 nm and power of around 1 mW, is launched into the tapered fiber to avoid the atoms sticking to the ONF surface [17]. The background photons induced by the 830 nm laser and the tweezer light are filtered out using a filter setup.

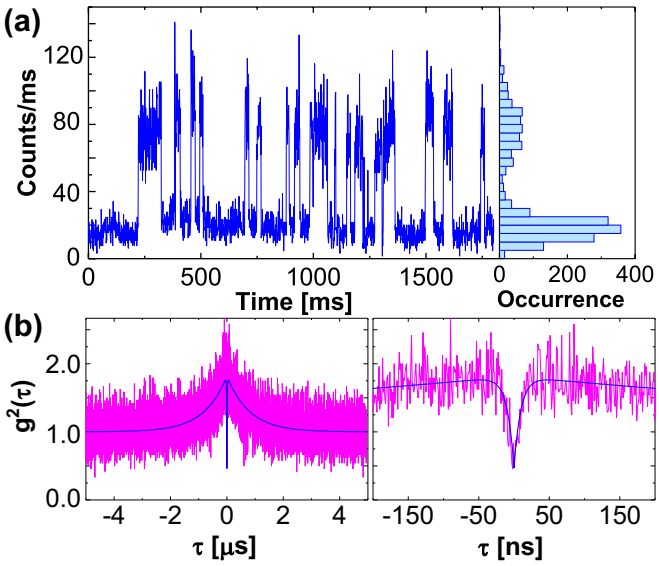

FIG. 2. (Color Online) (a) Real-time observation of trapped single atoms. The blue trace in the left panel shows the typical photon counts measured through the ONF cavity. The right panel shows the histogram of the photon counts. (b) Photon correlation of the ONF trap signal. The magenta trace shows the normalized correlation ($g^2(\tau)$) of the photon counts measured through the ONF cavity. The blue curve shows the theoretical fit. The right panel shows the enlarged view of the plot shown in the left panel.

The experiments are carried out by monitoring the photon counts through the ONF cavity while the tweezer beam is focused on the ONF and laser-cooled Cs-atoms are continuously loaded into the ONF-trap from a magneto optical trap (MOT). The typical photon counts measured through the ONF cavity, is shown in the left panel of Fig. 2(a). The right panel shows the histogram of the photon counts. It may be seen that discrete step-like signals with a height of 62±13 counts/ms are observed above a background of 17±7 counts/ms. The typical temporal duration of the step-like signal ranges from 10 to 100 ms. The signal resembles the single atom fluorescence signal measured in a conventional tightly focused dipole trap operating in collisional blockade regime [18]. It disappears when the tweezer beam or the repump beam of the MOT is switched off. This clearly indicates that

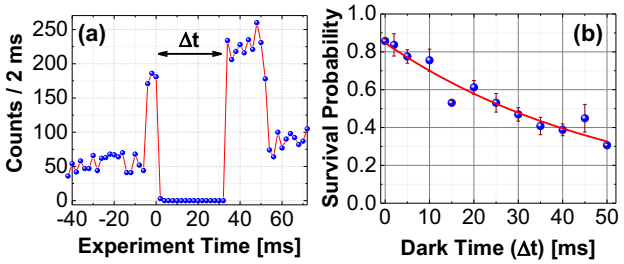

FIG. 3. (Color Online) Lifetime of the ONF-trap. (a) A typical experimental event. The blue dots show the measured photon counts in each time-bin (2 ms) and the red trace is just a guide to eye. (b) The measured survival probabilities plotted as a function of different dark times (Δt). The blue dots show the measured data with error-bars and the red curve shows the exponential fit to the data.

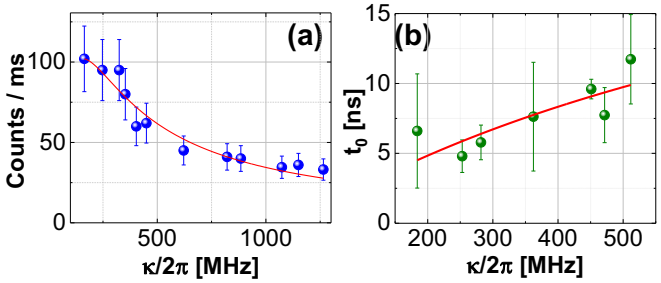

FIG. 4. (Color Online) Photon statistics of the fluorescence signal for different cavity modes. (a) The measured fluorescence counts plotted against the linewidths ($\kappa/2\pi$) of the cavity modes. The blue dots show the measured data with error-bars and the red curve shows the theoretical fit to the data. (b) The estimated rise time of the antibunching signal (t_0) plotted against the cavity linewidths. The green dots show the measured data with error-bars and the red curve shows the theoretical fit to the data.

single atoms are trapped and interfaced to the ONF cavity. The efficient channeling of the trapped single atom fluorescence into the ONF guided modes enables the real-time observation of the step-like fluorescence signal.

We have carried out photon correlation measurements of the fluorescence signal to further clarify the atom number and the dynamics of the trap. The magenta traces in Fig. 2(b) show the typical normalized photon correlation signal ($g^2(\tau)$) measured through the ONF cavity. The correlation signal shows anti-bunching behavior with $g^2(0) \simeq 0.47$. The anti-bunching of the fluorescence signal, confirms that indeed single atoms are trapped on the ONF. It should be noted that $g^2(0) > 0$ is due to the presence of background light scattered from the MOT beams into the ONF cavity. It may be seen that apart from the central anti-bunching dip the correlation signal shows a bunching behavior in longer time-scales. In order to further understand the behavior of the correlation signal, we fit the correlation signal using a model (see e.g. [6, 19]) given by

$$g^2(\tau) = 1 - (1 + C_0)e^{-\frac{|\tau|}{t_0}} + C_1 e^{-\frac{|\tau|}{t_1}} \qquad (1)$$

where t_0 and t_1 describes the characteristic time-scales of the anti-bunching and bunching signals, respectively. The coefficient C_1 describes the amplitude of the bunching signal and $(C_1 - C_0)$ gives the value of $g^2(0)$. The blue curve in Fig. 2(b) shows the fitting using the above model. From the fit, we estimate the parameters t_0, t_1, C_0 and C_1 to be 9.6±0.7 ns, 800±10 ns, 0.35±0.10 and 0.82±0.01, respectively. It should be noted that the t_0 may correspond to the cavity enhanced decay rate of the atom. On the other hand, the t_1 indicates a clustering of the photon emission into the cavity mode [6].

The real-time observation of single atoms trapped on the ONF enables various experiments to be performed in a deterministic way. Once a single atom is trapped on the ONF, a step-increase in the photon counts is observed through the ONF. This step-like signal can be used to trigger any experimental sequence. As a demonstration experiment, we present the lifetime measurement of the trapped single atoms on the ONF.

A typical measurement event is shown in Fig. 3(a). It may be seen that the presence of a single atom in the trap was inferred from the sudden rise in the photon counts and the experiment was triggered at 0 ms time. There was a dark-period (Δt) of 32 ms during which the MOT beams were switched off. After the dark-period, the MOT beams were switched on again to detect the presence of the atom in the trap. A high level of photon counts after the dark-period indicates that the atom was still present in the trap. The blue dots in Fig. 3(b), show the survival probabilities for different dark times (Δt). The red curve shows the exponential fit. From the fit, the trap lifetime is estimated to be 52±5 ms.

The data presented in Figs. 2 and 3, were measured for a cavity mode with a linewidth of 450 MHz. In order to estimate the cavity QED characteristics of the coupled atom-cavity system, we have analyzed the photon statistics of the fluorescence signal for different cavity modes. The measured fluorescence counts (height of the step-like fluorescence signal) are plotted against the linewidths of the cavity modes in Fig. 4(a). It may be seen that the fluorescence counts increases with decreasing cavity linewidth. We fit the data using the following relation (see e.g. [6, 20])

$$n_p = \alpha \frac{\Omega^2}{\gamma_0 C} \frac{|C'|^2}{|1 + C'|^2} \qquad (2)$$

where n_p is the fluorescence photon counts and $C' = g_0^2/[(\kappa/2 - i\Delta_c)(\gamma_0/2 - i\Delta_a)]$ is the complex cooperativity parameter. Here g_0, κ ($= 2\pi \times \Delta\nu$) and γ_0 ($= 2\pi \times 5.2$ MHz), are the atom-cavity coupling rate (single photon Rabi frequency/2), the decay rate of the cavity intensity and the free-space decay rate of atomic population, respectively. Ω, Δ_c ($= 0$ MHz) and Δ_a ($\simeq -3\gamma_0$) are the driving field's (MOT cooling beams) Rabi frequency and detunings from the cavity and atomic resonances,

respectively. $C = 4g_0^2/(\kappa\gamma_0)$ is the on-resonance single atom cooperativity. The experimental detection efficiency is described by the proportional factor α. From the fit, the atom-cavity coupling rate is estimated to be $g_0/2\pi = 34\pm2$ MHz. It should be noted that α and Ω are just proportional factors and assuming the experimentally obtained detection efficiency $\alpha = 4\%$ [17], the driving Rabi frequency is estimated to be $\Omega/2\pi = 5.4 \pm 0.2$ MHz which is comparable to that estimated from the MOT beam intensity.

We have also analyzed the photon correlation signal for different cavity modes. Figure 4(b) shows the estimated rise time of the antibunching signal (t_0) plotted against the cavity linewidths. It may be seen that t_0 increases with increasing cavity linewidth. We fit the data using a relation $t_0 = 1/(P_0\gamma_0 + 4g_0^2/\kappa)$, where $P_0 \simeq 1.044$ is the Purcell factor due to the ONF in the absence of the cavity [7, 8, 16]. From the fit, the atom-cavity coupling rate is estimated to be $g_0/2\pi = 36\pm1$ MHz, which is in reasonable agreement with analysis of Fig. 4(a).

It should be noted that due to proper selection of ONF diameter and trapping laser wavelength (magic wavelength), the fluorescence of single atoms trapped on the ONF can be directly observed in real-time above the scattering background from the MOT beams. The typical ONF diameter of 400-500 nm widely adopted in the reported experiments may not be suitable for the present trapping scheme [17]. The trap lifetime is similar to previously reported values for ONF based guided mode traps [10, 15]. The lifetime is mainly limited by the mechanical modes of the tapered fiber [21] and can be improved using Raman-cooling techniques [22].

From the estimated g_0, it is clear that the cavity modes presented here are operating in the Purcell regime of cavity QED. We have estimated a cooperativity of $C = 5.4\pm0.6$, a cavity-enhanced Purcell factor ($P = P_0 + C$) of 6.4 ± 0.6 and a cavity-enhanced channeling efficiency ($\eta_c = (P_0\eta + C)/(P_0 + C)$) of $85\pm2\%$ for the cavity mode with a linewidth of 164 MHz (corresponding to a finesse of $F = \Delta\nu_{FSR}/\Delta\nu = 140$) [7, 8]. It should be noted that from the cavity length, the atom-cavity coupling rate is estimated to be $g_0 = (cP_0\gamma_0\eta/L)^{1/2} = 2\pi \times 63 \pm 3$ MHz, where c is the speed of light in vacuum [7, 8]. This may be understood from the fact that the confinement of the trap along the axis of ONF is weak and due to the motion of the atom in the trap, it can transit between node and antinode of the cavity mode [23]. At the antinode (node) position the atom-cavity coupling rate and hence the photon emission rate into the cavity mode will be strongly enhanced (suppressed), respectively. As a result, the g_0 estimated from the photon statistics, is an averaged value. This is also evident from the bunching behavior of $g^2(\tau)$ resulting from the clustering of the photon emission into the cavity mode [23].

The axial confinement can be improved by further cooling the atoms [22] or by introducing a blue-detuned standing wave into the ONF guided mode (see e.g. [6, 24]). By confining the atom to the antinode position the cooperativity can be improved by a factor of $\sim$3.7. In principle, the cavity finesse can be improved to $F = 400 - 500$ as in Ref. [9] to further increase the cooperativity by another factor of $\sim$3. Such high cooperativity and faster out coupling rate, will be preferable for various quantum photonics applications like single photon generation, single photon switching and high fidelity atom-photon quantum gates [2, 4]. Aided with fiber-in-line capabilities, such ONF cavity will be a promising candidate among the existing state-of-the-art fiber-coupled quantum interfaces [2–6] for quantum photonics applications.

In summary, we have demonstrated that individual single atoms are trapped and efficiently interfaced to the ONF cavity, and can be readily observed in real-time through the fiber guided modes. These results may open new possibilities for deterministic preparation of single atom events for quantum photonics applications on an all-fiber platform. Moreover, with further developments the present trapping scheme can be extended to a moving tweezer based scheme [3, 4] to arrange a pair or an array of atoms on the ONF in any desired configuration with control over individual atom sites [25]. This type of few millimeter length ONF cavities will be particularly suitable to interface large arrays of single atoms to a single nanophotonic platform. This will open new avenues to engineer complex quantum systems for investigation of long-range atom-atom interaction mediated by the photonic mode [26] and entanglement based quantum gates [27].

ACKNOWLEDGMENTS

We acknowledge Kohzo Hakuta, Tetsuo Kishimoto and Makoto Morinaga for fruitful discussions. This work was supported by the Japan Science and Technology Agency (JST) as one of the Strategic Innovation projects. KPN acknowledges support from a grant-in-aid for scientific research (Grant no. 15H05462) from the Japan Society for the Promotion of Science (JSPS) and support from Matsuo Science Promotion Foundation, Japan. K. P. Nayak and J. Wang contributed equally to this work.

⋆ Corresponding Author: kalipnayak@uec.ac.jp

‡ wangjie605@126.com, Present Address: Center for Emergent Matter Science (CEMS), RIKEN, Wako, Saitama 351-0198, Japan.

[1] H. J. Kimble, Nature **453,** 1023 (2008).
[2] A. Reiserer and G. Rempe, Rev. Mod. Phys. **87,** 1379 (2015).
[3] J. D. Thompson, T. G. Tiecke, N. P. de Leon, J. Feist, A. V. Akimov, M. Gullans, A. S. Zibrov, V. Vuletic, and M. D. Lukin, Science **340,** 1202 (2013).
[4] T. G. Tiecke, J. D. Thompson, N. P. de Leon, L. R. Liu, V. Vuletic, and M. D. Lukin, Nature 508, 241244 (2014).
[5] C. Junge, D. OShea, J. Volz, and A. Rauschenbeutel, Phys. Rev. Lett. **110,** 213604 (2013).
[6] J. Gallego, W. Alt, T. Macha, M. Martinez-Dorantes, D. Pandey, and D. Meschede, Phys. Rev. Lett. **121,** 173603 (2018).
[7] F. L. Kien and K. Hakuta, Phys. Rev. A **80,** 053826 (2009).
[8] K. P. Nayak, M. Sadgrove, R. Yalla, F. L. Kien, and K. Hakuta, J. Opt. **20,** 073001 (2018).
[9] J. Keloth, K. P. Nayak, and K. Hakuta, Opt. Lett. **42,** 1003 (2017).
[10] S. Kato and T. Aoki, Phys. Rev. Lett. **115,** 093603 (2015).
[11] K. P. Nayak and K. Hakuta, Opt. Express **21,** 2480 (2013).
[12] K. P. Nayak, P. Zhang, and K. Hakuta, Opt. Lett. **39,** 232 (2014).
[13] F. L. Kien, V. I. Balykin, and K. Hakuta, Phys. Rev. A **70,** 063403 (2004).
[14] F. L. Kien, V. I. Balykin, and K. Hakuta, J. Phys. Soc. Jpn. **74,** 910 (2005).
[15] E. Vetsch, D. Reitz, G. Sague, R. Schmidt, S. T. Dawkins, and A. Rauschenbeutel, Phys. Rev. Lett. **104,** 203603 (2010).
[16] F. L. Kien, S. D. Gupta, V. I. Balykin, and K. Hakuta, Phys. Rev. A **72,** 032509 (2005).
[17] See Supplementary Material.
[18] N. Schlosser, G. Reymond, and P. Grangier Phys. Rev. Lett. **89,** 023005 (2002).
[19] S. C. Kitson, P. Jonsson, J. G. Rarity, and P. R. Tapster, Phys. Rev. A **58,** 620 (1998).
[20] Y. H. Lien, G. Barontini, M. Scheucher, M. Mergenthaler, J. Goldwin, and E. A. Hinds, Nature Communications **7,** 13933 (2016).
[21] D. Hmmer, P. Schneeweiss, A. Rauschenbeutel, and O. Romero-Isart, arXiv:1902.02200 (2019).
[22] Y. Meng, A. Dareau, P. Schneeweiss, and A. Rauschenbeutel, Phys. Rev. X **8,** 031054 (2018).
[23] It should be noted that all data presented here except Fig. 2(b), were measured for a trap depth of 0.9 mK. For the $g^2(\tau)$ measurement (shown in Fig. 2(b)) the trap depth was increased to $\sim$2.6 mK to get better signal to noise ratio. This corresponds to a trap frequency of $2\pi\times$ 136 kHz along the ONF axis. From the observed t_1-value and considering the separation of 211 nm between the node and antinode, we estimate the effective temperature of the atoms in the trap to be 0.55 mK. This yields a spatial extent of the trap [28] of 218 nm along the ONF axis which is comparable to the node-antinode separation. See Supplementary Materials [17] for details.
[24] M. Khudaverdyan, W. Alt, I. Dotsenko, T. Kampschulte, K. Lenhard, A. Rauschenbeutel, S. Reick, K. Schrner, A. Widera and D. Meschede, New J. Phys. **10,** 073023 (2008).
[25] M. Endres, H. Bernien, A. Keesling, H. Levine, E. R. Anschuetz, A. Krajenbrink, C. Senko, V. Vuletic, M. Greiner, and M. D. Lukin, Science **354,** 1024 (2016).
[26] F. L. Kien, S. Dutta Gupta, K. P. Nayak, and K. Hakuta, Phys. Rev. A **72,** 063815 (2005).
[27] S. Welte, B. Hacker, S. Daiss, S. Ritter, and G. Rempe, Phys. Rev. X **8,** 011018 (2018).
[28] R. Grimm, M. Weidemller, and Y. B. Ovchinnikov, Adv. At., Mol., Opt. Phys. **42,** 95 (2000).